Nucleophilic covalent ligand discovery for the cysteine redoxome

Ling Fu[1,4], Youngeun Jung[2,4], Caiping Tian[1,3], Renan B. Ferreira[2], Fuchu He[1,3], Jing Yang[1]*

and Kate S. Carroll[2]*

[1]State Key Laboratory of Proteomics, Beijing Proteome Research Center, National Center for

Protein Sciences • Beijing, Beijing Institute of Lifeomics, Beijing 102206, China

[2]Department of Chemistry, UF Scripps Biomedical Research, Jupiter, Florida 33458

[3]School of Medicine, Tsinghua University, Beijing 100084, China

[4]Authors contributed equally to this work

*e-mail: yangjing@ncpsb.org.cn

*e-mail: kate.carroll@ufl.edu

The convergence of reactive cysteine-targeted electrophilic fragments and chemoproteomics have dramatically accelerated the discovery of ligandable sites in the proteome. Our genome encodes 214,000 cysteine residues, at least 20% of which are estimated to be redox-active. Oxidation blunts sulfur reactivity toward electrophiles but opens the door to a new class of nucleophilic covalent ligands that target cysteinyl sulfenic acids, which are widespread post-translational modifications. Here we report a quantitative analysis of nucleophilic fragments screened against the human sulfenome. Ligands were discovered for >500 sulfenated cysteines in >400 proteins, including sites not targeted by electrophiles with the same scaffold. Among these were compounds that preferentially react with hepatoma-derived growth factor (HDGF)-related proteins (HRPs) one of which was able to block nuclear transport of this oncoprotein. Nucleophilic fragments provide a rich resource for chemical biology and drug discovery, where ligandability in the human proteome extends beyond protein thiols.

Main

Targeted covalent inhibitors[1] and degraders[2] have emerged as a promising therapeutic class

for various indications, particularly for the treatment of cancer. Covalent drugs have been

successfully applied to key oncogenic driver proteins, including EGFR and mutant KRAS,

historically considered to be "undruggable"[3]. Despite encouraging results in the clinic, much

of the human proteome still lacks defined small-molecule ligands and the number of "hot spots"

identified for covalent targeting remains limited. The need to expand the protein landscape

that is amenable to targeting by covalent chemistry is significant and various approaches have

been reported to access chemical functionality inherent to amino acid side chains. Up to now,

these efforts have been directed toward cysteine[4,5] and other nucleophilic residues, including

lysine[6], tyrosine[7], and aspartate[8]. In general, covalent inhibitors contain an electrophilic

group or "warhead" connected a small-molecule fragment and libraries of such compounds

have been screened to identify novel ligands of the human proteome.

Among the amino acids targeted by residue-specific chemistry, cysteine is most nucleophilic[9].

Although the frequency of cysteine in the human proteome is only ~3.3% it constitutes more

than 20% of Uniprot-annotated enzyme active site residues[10]. Owing to its unique chemical

reactivity and prevalence in functional sites of proteins, cysteine has thus far emerged as the

predominant target in covalent drug discovery[3,11]. Almost all targeted covalent inhibitors

(TCIs) approved by the FDA as drugs or as candidates in clinical trials are designed to target

reduced form of cysteine (*i.e.,* thiols or thiolates) located at a functional site in therapeutically

important proteins[12]. Examples include afatinib[13] and ibrutinib[14] that target cysteines in the

catalytic pocket of the epidermal growth factor receptor (EGFR) and Bruton tyrosine kinase (BTK), respectively.   Combined with chemoproteomic strategies, such as activity-based protein profiling (ABPP)[15], thiol-directed electrophilic fragments have been mined to expand the ligandable space in human cysteinomes[5].   One elegant application of this approach has led to the discovery of compounds that suppress T cell activation and promote the degradation of immunomodulatory proteins[16], further highlighting the potential of cysteine-targeted covalent fragment libraries as viable starting points for the development of chemical probes and drugs.

Cysteine residues are also subject to diverse redox chemistry in cells through reaction with exogenous and endogenous reactive oxygen/nitrogen species (RO/NS)[17].   Consequently, the chemical reactivity of the cysteinome extends well beyond the reduced, thiol state. Although an array of redox modifications to cysteine are possible, sulfenic acid (–SOH) is the most widespread by far and has been mapped by chemoproteomics in thousands of proteins in cells and tissues[18–20].   This cysteine "oxoform" is formed by oxidation of a thiolate by ROS such as hydrogen peroxide (H_2O_2) produced during signaling and metabolism or by hydrolysis of sulfenyl halides, nitrosothiols, and polarized disulfides[21].   If stabilized by the microenvironment, a thiol-sulfenic acid pair can operate as a regulatory redox switch.   For example, site-specific oxidation of cysteinyl thiols to sulfenic acid enhances the activity of EGFR[22,23] and Src[24] kinases.   Conversely, enzymes that require a thiolate for catalysis like protein tyrosine phosphatases (PTPs) are inhibited by oxidation[25] and oxidation of cysteines in allosteric sites of proteins is also well-known[26].

Apropos to covalent targeting and fragment-based ligand discovery, the sulfur atom of sulfenic acid is distinguished from other thiol modifications by moderate electrophilic reactivity[21]. In this state, the chemical reactivity of sulfur toward electrophiles is orders of magnitude less than its thiol counterpart and, consistent with this fact, we have shown that chronic oxidative stress leads to the formation of an EGFR subpopulation that is refractory to afatinib treatment in cells[22,27]. Elevated ROS is associated with many diseases[28] including cancer[29], diabetes[30], and Pakinson's[31]. Thus, it is logical to expect that oxidized forms of cysteine accumulate in proteins over time and that these modifications will affect the pharmacology of covalent drugs that target this residue in its reduced form.

With an eye to developing new chemical methods for covalent ligand discovery, we posited that the unique electrophilic sulfur atom in sulfenic acid can serve as the novel reaction partner. Although the use of nucleophilic fragments is a relatively new idea, earlier proof-of-concept studies, have shown promising results including the discovery of covalent inhibitors that target the oxidized PTP active site[32,33] and exploration of C-nucleophile chemical reactivity through site-centric chemoproteomics[34]. While intriguing, these studies don't really begin to scratch the surface of the landscape of ligandable, oxidized cysteines in the human proteome[19]. Herein, we have adapted a quantitative chemoproteomic platform termed SulfenQ[20] to quantify intrinsic reactivity of protein sulfenic acids and systematically screened a curated nucleophile fragment library against the human sulfenome (>8,200 sites in total) in the native proteome. This large-scale analysis leads to the discovery of redox-sensitive sites that can

be targeted by covalent ligands to perturb function across a wide range of proteins, including

those not targeted by thiol-reactive fragments even those with the same binding scaffold.

Results

Quantitative profiling intrinsic cysteinyl sulfenic acid reactivity in the human proteome.

In previous work, we have described a ratiometric quantification method termed 'SulfenQ' that

measures relative changes across the sulfenome in lysates or cells[20].   Building on this work,

we first adapted this approach to globally quantify intrinsic electrophilic reactivity of cysteinyl

sulfenic acids by dose-dependent proteome labeling with the "clickable" sulfenic acid-selective

probe, BTD[35,36] (Fig. 1a).   This strategy is analogous to that used to assess nucleophilic

cysteine[9] and lysine[6] reactivity and is based on the principle that so-called "hyperreactive"

sulfenic acids will be quantitively labeled at low BTD concentrations, while less reactive sites

will exhibit concentration-dependent increases in probe labeling (Fig. 1b).

To test this concept, we prepared native lysates from MDA-MB-231 cells and treated with 0.5

or 5 mM of BTD for 2 h.   BTD-labeled proteomes were subsequently digested and clicked to

isotopically differentiated biotin for enrichment, identification, and quantification.   Cysteinyl

sulfenic acids with a heavy to light ratio ($R_{H/L}=R_{10:1}$) below 2.0 were empirically designated

"hyperreactive", those with $R_{10:1}$ values higher than 2.0 but not greater than 5.0 were

designated as "moderately reactive", and those with $R_{10:1}$ values higher than 5.0 as sites

having "low reactivity".   In parallel, control experiments to minimize bias in quantification were

performed in which lysates were treated with the same BTD concentration (*i.e.,* 5 mM versus

6

5 mM).   High-confidence quantifiable sulfenic acid sites were required to be detected in both

10:1 and 1:1 data sets with the later R value in the range of 0.67-1.5 (Supplementary Fig. 1a-

c).
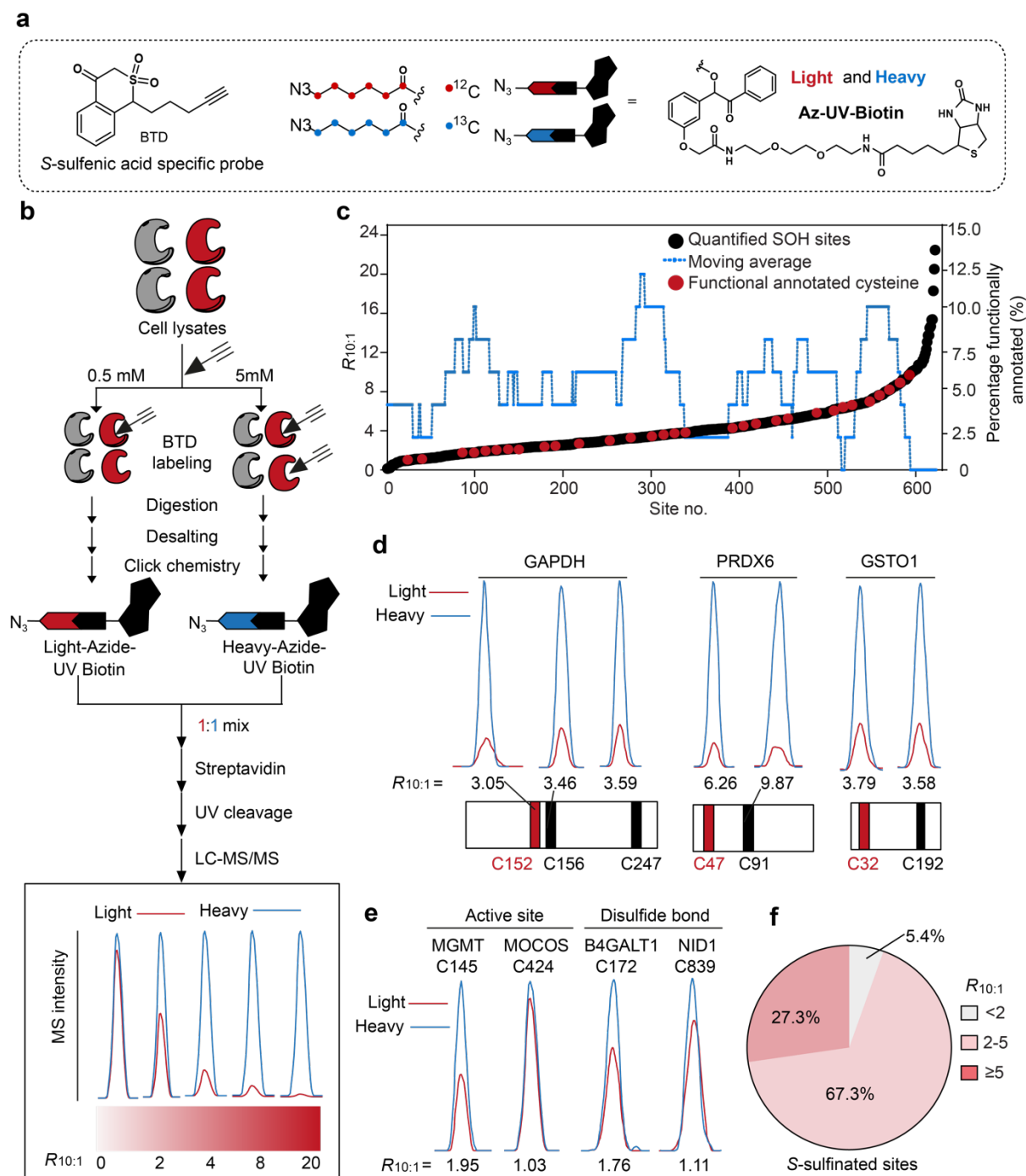
Fig. 1. Quantitative profiling of intrinsic SOH-reactivity in the human proteome.   a, Chemical structures of a 'clickable' sulfenic acid-specific probe, BTD, and isotopically labeled azide-biotin reagents with a photocleavable linker (Az-UV-biotin).   **b,** Quantitative chemoproteomics for site-specific quantification of the intrinsic reactivity of cysteine sulfenic acids in a human MDA-MB-231 breast cancer cell line proteome.   MDA-MB-231 cell lysates were labeled with 0.5 mM and 5 mM BTD, respectively, and digested by trypsin.   The resulting BTD-modified peptides were conjugated to light and heavy Az-UV-biotin, respectively, *via*

click chemistry. The light and heavy labeled samples then were mixed equally in amount and subjected to streptavidin-based enrichment. After several washing steps, the modified peptides were selectively eluted from beads under 365 nm wavelength UV light for LC-MS/MS-based proteomic analysis. **c,** Correlation of $R_{10:1}$ values with functional annotations from the UniProt database, where active sites, disulfide bonds, or metal binding sites are shown in red, and all other quantified sulfenic acid sites in black. A moving average line of functional annotated sites is shown in a dashed blue line. **d-e,** Representative extracted ion chromatograms (XICs) showing changes in BTD-labeled peptides from known redox-sensitive proteins (**e**) and those bearing functionally important cysteines (**f**). Profiles for light- and heavy-labeled peptide are shown in red and blue, respectively. The average $R_{10:1}$ values calculated from four biological replicates are displayed below each XIC. **f,** Pie chart showing the percentage of previously identified *S*-sulfinated (–SO_2H) sites across the intrinsic sulfenic acid reactivity ranges.

In total, we were able to calculate $R_{10:1}$ for 622 cysteinyl sulfenic acid sites across 477 proteins (Fig.1c and Supplementary Data 1). A subset (121 or 19.5%) was hyperreactive, exhibiting dose-independent BTD reactivity ($R_{10:1}<2.0$); the majority (319 or 51.3%) were moderately reactive, while the remainder (182 or 29.3%) were characterized as having low reactivity ($R_{10:1}>5.0$). In general, proteins identified in this study harbored a single "reactive" sulfenic acid among several quantified sites within the same polypeptide (Supplementary Fig. 1d-e). Unlike hyperreactive thiols, hyperreactive sulfenic acids were not significantly enriched in cysteines with annotated nucleophilic functions (*e.g.,* active-site, disulfide, metal binding) across the UniProt Knowledgebase[10] (Fig. 1d). For example, sulfenic acids in the active sites of several well-characterized redox proteins, including GAPDH C152, PRDX6 C47 and GSTO1 C32, exhibited moderate to low reactivity. Some interesting exceptions to this observation were, however, identified (Fig. 1e) including the active site cysteines of the DNA methyltransferase, MGMT ($R_{10:1}=1.95$) and the molybdenum cofactor sulfurase, MOCOS and ($R_{10:1}=1.03$) and disulfide cysteines in the galactosyltransferase, B4GALT1 ($R_{10:1}=1.76$) and glycoprotein, NID1 ($R_{10:1}=1.11$). Comparing these data sets with previously mapped sites of sulfinic acid (–SO_2H) modification[37] reveals that sulfination (i.e., overoxidation) is more likely to occur at sulfenic acids with at least moderate intrinsic reactivities (Fig. 1f).

Next, we asked whether the intrinsic reactivity of the sulfur in cysteinyl sulfenic acid correlated to the intrinsic reactivity of cysteinyl thiols mapped in an earlier study[4]. In fact, no significant correlation between these features was observed (r=0.12; Supplementary Fig. 2a). While seemingly trivial, this analysis illustrates the fundamental difference in chemical reactivity between cysteine and a closely related "oxoform"; namely, the sulfur in hyperreactive thiols is nucleophilic and in hyperreactive sulfenic acids is uniquely electrophilic. For instance, active site GSTO1 C32 is hyperreactive in its thiol form but shows only modest sulfenic acid reactivity (Supplementary Fig. 2b). Likewise, the thiol form of GAPDH C247 has low reactivity, and its sulfenic acid form is moderately reactive (Supplementary Fig. 2b). An important corollary to these observations is that cysteines thiols identified as hyperreactive are not necessarily redox-sensitive. Together, these observations clearly establish the disparate reactivity within the human cysteinome and sulfenome.

Electrophilic and nucleophilic fragments with the same binding scaffold have distinct target profiles. Next, we sought to compare the ligandability of compounds with the same binding scaffold but with warheads of nucleophilic or electrophilic reactivity against both sub-proteomes (Fig. 2a). To profile the cysteinome, we selected chloroacetamide and acrylamide warheads (**1** and **2**, Fig. 2b, inset) which have been widely used in covalent fragments ligand and drug discovery[38]. To profile the sulfenome, we selected cyanoacetamide C-nucleophile, **3a** previously reported by our group to have moderate, selective reactivity with sulfenic acid[39] and nitroacetamide, **3b**. In these studies, we employed linear C-nucleophiles, as opposed to cyclic analogs, to minimize differences in cysteine ligandability due to gross structural

differences between thiol- and sulfenic-acid reactive warheads.   Of note, compounds **3a** and

3b differ in the stability of their covalent link to sulfur.   The thioether formed between sulfenic

acid sulfur and cyanoacetamides is covalent, but reversible ($t_{1/2}$ ~2 h) whereas the same

linkage to nitroacetamides is considerably more stable ($t_{1/2}$ >24 h) (Supplementary

Information).   Thiol- and sulfenic acid-reactive groups were linked by amide bond formation

to a commercially available 3,5-bis(trifluoromethyl)aniline fragment with validated ligandability

throughout the cysteinome[4].   Electrophilic fragment-cysteinyl thiol-ligand interactions were

subsequently measured using a quantitative chemoproteomic platform known as QTRP[40]

(quantitative thiol reactivity profiling), while nucleophilic fragment-cysteinyl sulfenic acid-ligand

interactions were measured using SulfenQ[18,20] in a pseudo-competitive format (Fig. 2a).

Native lysates from MDA-MB-231 cells were treated with fragment or vehicle (500 µM for **1**

and **2**, 2 mM for **3a** and **3b**), followed by thiol- or sulfenic acid-reactive probe (100 µM of IPM

or 5 mM BTD).   Note that fragment and BTD concentrations were increased relative to their

thiol-reactive counterparts to compensate for the lower abundance of sulfenic acids in the

human proteome.   Fragment-sensitive sites, hereafter referred as to "liganded sites" were

defined as those exhibiting at least a 4-fold reduction (≥75%) in IPM or BTD labeling efficiency

in the presence of each fragment compared to DMSO control ($R_{H/L}=R_{DMSO/Fragment}≥4$).

Overall, we quantified >5,300 thiol and >2,300 sulfenic acid sites from 3,856 proteins across

all datasets (Fig. 2b and Supplementary Data 2).   Among the quantifiable cysteine thiols were

1,100 and 580 liganded sites, corresponding to a ligand rate (the percentage of liganded sites

relative to total sites for each fragment) of 25.2% and 11.0% for **1** and **2**, respectively (Fig. 2c
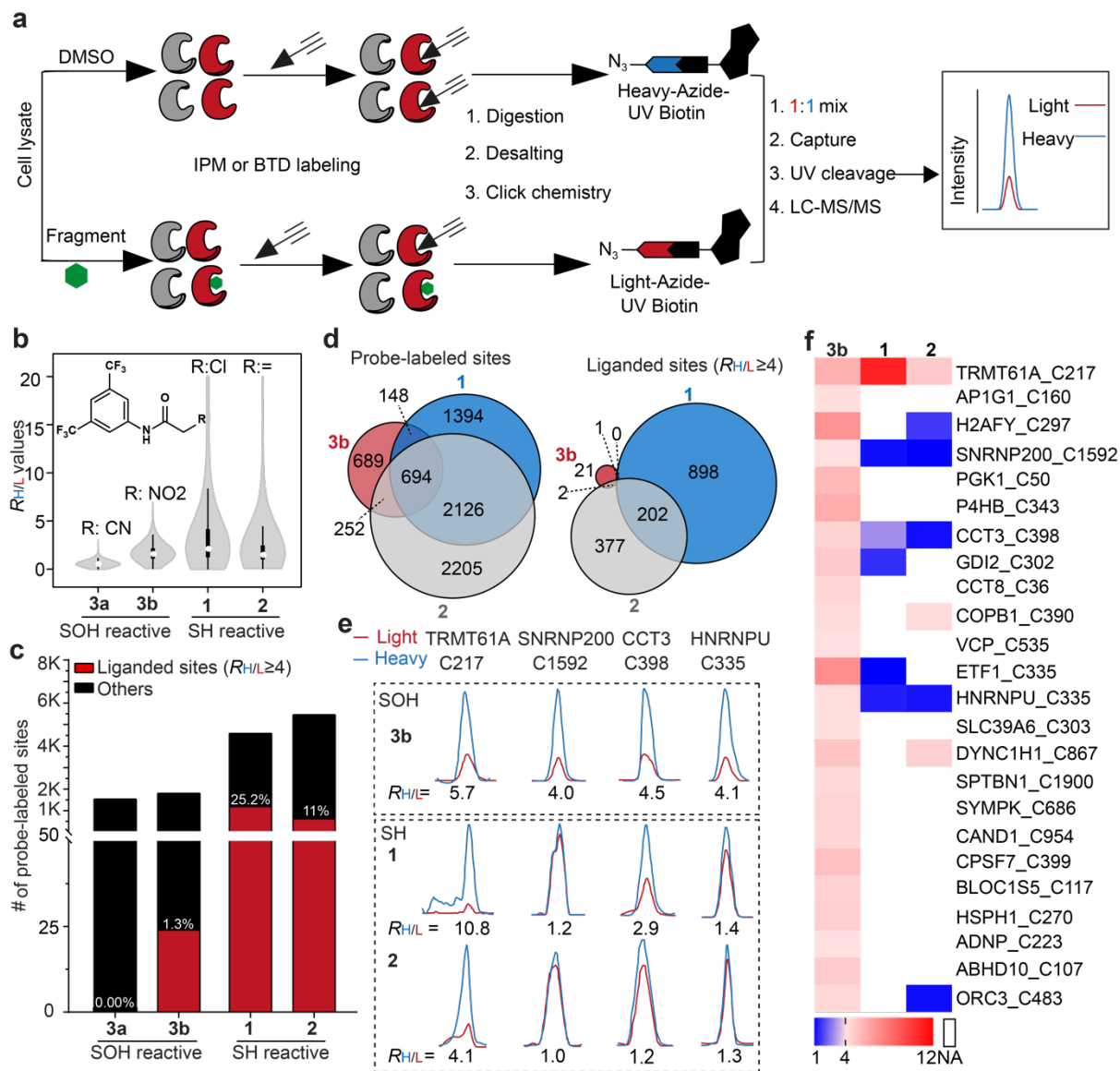
Fig. 2. Distinct target profiles of electrophilic and nucleophilic fragments with the same scaffold. **a,** Chemoproteomic target profiling of electrophilic and nucleophilic fragments in a human MDA-MB-231 breast cancer cell line proteome. MDA-MB-231 cell lysates were treated with either fragment or vehicle, respectively, and labeled with the probe as indicated (BTD for nucleophiles and IPM for electrophiles). Probe-labeled proteomes were digested by trypsin and the resulting probe-modified peptides were conjugated to light or heavy Az-UV-biotin *via* click chemistry. Light and heavy labeled samples then were mixed equally in amount and subjected to streptavidin-based enrichment. After several washing steps, the modified peptides were selectively eluted from beads under 365 nm wavelength UV light for LC-MS/MS-based proteomic analysis. **b,** Distribution of $R_{H/L}$ values of each fragment across the MDA-MB-231 sulfenome (**3a** and **3b**) or cysteinome (**1** and **2**). **c,** Bar chart showing the numbers of –SH or –SOH sites liganded by each fragment. Percentage of liganded sites is shown on each bar. **d,** Venn diagrams showing the overlap of overall quantified cysteine sites in either sulfenated form or reduced form (left) and the liganded ones by fragments as indicated (right). **e,** Representative XICs showing changes in probe-labeled peptides from proteins as indicated. The profiles for light- and heavy-labeled peptide are shown in red and blue, respectively. The average $R_{H/L}$ values calculated from biological duplicates are displayed below each XIC. **f,** Heat map showing representative fragment interactions for liganded cysteines in either sulfenated (–SOH) or reduced (–SH) forms.

and Supplementary Fig. 3). In contrast to the high number of liganded thiols identified, only

24 sulfenic acid sites were liganded by nucleophilic fragment, **3b**, corresponding to a ligand

rate of 1.3%, while **3a** did not yield any detectable liganded sites (Fig. 2c). A control fragment

lacking the reactive warhead was also screened and showed negligible proteome reactivity (**4**, 0.05%; Supplementary Data 2).   The absence of ligandability by compound **4** indicates that liganded sites likely reflect covalent interaction.   We were initially discouraged by the lack of liganded sites identified by **3a**, studies of ligand reversibility quickly indicated that this was most likely uniquely due to the presence of two strong electron-withdrawing $-CF_3$ substituents. Although both thiol and sulfenic acid states were mapped onto >1,000 cysteines, only three were liganded by both electrophilic and nucleophilic fragments (Fig. 2d).   On such example is C217 of tRNA methyltransferase, TRMT61A, which was liganded by **1**, **2** and **3b** (Fig. 2e). We also identified a small cohort of cysteines that were exclusively liganded by **3b** (Fig. 2e,f) including C1592 of the small nuclear riboprotein, SNRNP200, C398 of T-complex protein, CCT3 and C335 of the heterogeneous riboprotein, HNRNPU.   These findings suggest that the human sulfenome has a smaller, but distinct ligandable space compared to the cysteinome.

Global analysis of nucleophilic fragment- sulfenic acid interactions.   Encouraged by the pilot study above, we next prepared nucleophilic analogs of the electrophilic fragment library reported in 2016[4] (cyanoacetamides: **5a-30a**, **35-41** and nitroacetamides: **5b-30b** and **42-43**; Supplementary Fig. 4).   Synthesis of cyanoacetamides from cyanoacetic acid was generally straightforward by EDC activation or *in situ* generation of the acid chloride and coupling to the corresponding amine.   The preparation of nitroacetamides proved more challenging owing to the unstable nature of nitroacetic acid.   Since standard amide coupling conditions could not be used for this series, several methods for nitroacetamide preparation were developed. Some compounds could be prepared by converting the nitroacetic acid to the acid chloride

followed by treatment with the amide. If this was unsuccessful, we employed bis(methylthio)-2-nitroethane as a masked carbonyl that could undergo addition-elimination with the desired amine. Still other nitroacetamide fragments were prepared from bromoacetyl bromide coupled the amine followed by installation of the nitro using a sodium iodide in combination with silver nitrite.

With the nucleophilic-fragments in hand, the 65-member library was screened against sites of basal sulfenic acid modification in the human proteome. In total, we quantified 8,235 BTD-labeled sites in 3,793 proteins (Supplementary Data 3). Among these, 4,845 (58.82%) sites were quantified in biological duplicates with a coefficient of variation (CV) less than 40%, underscoring the reproducibility of our method. On average, 1,958 BTD-labeled sites were quantified per dataset with medium CV values ranging from 4.11% to 11.2% and 6,132 (74.5%) cysteines were quantified in at least three fragment datasets (Supplementary Fig. 5). The nucleophilic-fragment library exhibited noteworthy differences in target reactivity across the human sulfenome, with most showing liganded rates (also referred as to sulfenome reactivity) of <1.0%; only a single compound, **5b**, had a significantly higher rate (20%; Fig. 3a,b). For example, C25 of the transport protein, SEC61G was liganded by nitroacetamide **5b** and not closely related analogs **3b** or **9b** (Fig. 3c). Likewise, C150 of a peptidase TPP2 was liganded by cyanoacetamides **5a** and not closely related analogs **3a** or **9a** (Supplementary Data 3).
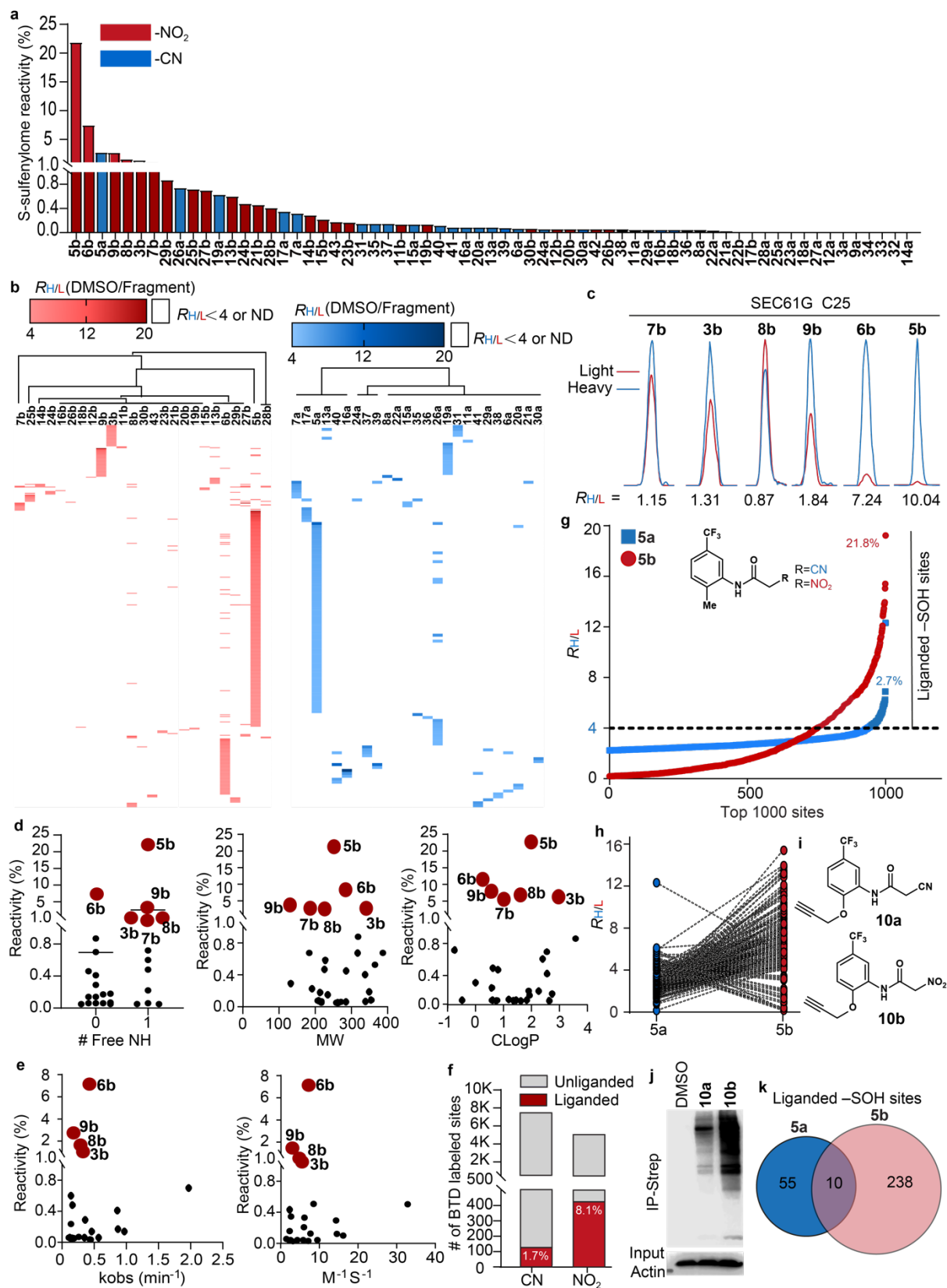
Fig. 3. Global analysis of nucleophilic fragment-sulfenic acid interactions. **a,** Bar chart showing the sulfenome reactivity values (also referred as to liganded –SOH rates) of nucleophilic fragments calculated as the percentage of all quantified –SOH sites with $R_{H/L}$ values ≥4 for each fragment. MDA-MB-231 cell lysates were treated with either fragment or vehicle, respectively, and labeled with BTD. The probe-labeled proteomes were processed and analyzed as aforementioned for obtaining $R_{H/L}$ values of each profiled SOH site. **b,** Heat maps showing $R_{H/L}$ values ($R_{H/L}$≥4) of all –SOH sites liganded by nitroacetamide (left) and cyanoacetamide (right)-based nucleophile fragments, respectively. ND: not detected. **c,** Representative XICs showing

14

changes in BTD-labeled peptides from SEC61G.   The profiles for light- and heavy-labeled peptide are shown in red and blue, respectively.   The average $R_{H/L}$ values calculated from biological duplicates are displayed below each XIC.   **d,** Scatter plots showing correlation of sulfenome reactivity of each nitroacetamide fragment with the corresponding structural features, including number of free NH (left), molecular weight (MW, middle), and CLogP value (right).   **e,** Scatter plots showing correlation of sulfenome reactivity of each nitroacetamide fragments with the corresponding kinetic parameters, including the observed binding constant (k_{obs}, left) and rate constant ($M^{-1}s^{-1}$, right).   **f,** Bar chart showing the number of –SOH sites liganded by nitroacetamide and cyanoacetamides nucleophile fragments.   **g,** Rank plot of $R_{H/L}$ (DMSO versus fragment) values of two representative fragments, **5a** and **5b**.   **h,** Line series plot showing the comparison of $R_{H/L}$ values obtained from common sites in the **5a** and **5b** dataset.   Only liganded sites obtained in either of two datasets are shown.   **i**, Alkyne analogs of **5a** and **5b**.   **j,** Western blot showing overall sulfenated proteins labeled by **10a** and **10b**, respectively.   Cells were treated with each probe as indicated for 1 h.   Cell lysates were harvested, clicked with azide-biotin, separated by SDS-PAGE, and detected using an antibody against streptavidin.   **k,** Venn diagram showing the overlap of liganded –SOH sites by **5a** and **5b**.

Next, we systematically investigated the relationship between structural features of recognition scaffolds and sulfenome reactivity.   In general, nitroacetamide fragments with free NH groups displayed higher sulfenome reactivity than those without, while no apparent impact of molecular weight and CLogP was observed on liganded rates (Fig. 3d).   Furthermore, given the relatively minor contribution from the "targeting" portion of the fragment on nucleophile reactivity (Fig. 3e and Supplementary Fig. 4), observed differences in ligandability are most likely attributed to binding energy imparted the unique scaffold.   Similar observations were made for cyano-acetamide fragments (Supplementary Fig. 6a-c).

Nitroacetamide fragments generally exhibited higher liganded rates compared to cyanoacetamide analogs (8.1% versus 1.7%; Fig. 3f and Supplementary Fig. 7).   Amongst different scaffolds, *m*-trifluoromethyl *o*-methylphenyl **5a** and **5b** showed relatively high liganded rates across the sulfenome, yielding 248 and 61 liganded sites, respectively (Fig. 3g). Although **5a** and **5b** often targeted the same sites, the former was generally less potent (2.7% versus 21.8%; Fig. 3h), albeit with interesting exceptions.   The difference in liganded rates between cyano- and nitroacetamide fragments is most simply attributed to the increased stability of the nascent thioether of the latter.   Broadly reactive fragments such as **5a** and **5b** are commonly referred to "scouts"[41].   To independently substantiate sulfenome reactivity of

fragments **5a** and **5b** we synthesized the *O*-propargyl alkyne analogs, **10a** and **10b** (Fig. 3i) and used these probes to label the sulfenome.   Both fragments were indeed broadly reactive, with fragment **10b** exhibiting greater proteome labeling compared to **10a** (Fig. 3j and Supplementary Fig. 8).   Putting the phrase "broadly reactive" across the sulfenome into context with the cysteinome, ~3.7% of proteins with sulfenated cysteines detected by BTD contained cysteines liganded by both **5a** and **5b** (Fig. 3k).

Overall, the cyano- and nitroacetamide fragment libraries provided 524 liganded sites in 441 proteins, corresponding to 6.3% and 11.6% of the total mapped sites and proteins, respectively. This profile is distinct from that liganded by electrophilic fragments (Supplementary Fig. 9a). Comparing the liganded dataset with intrinsic reactivity, hyperreactive sulfenic acids showed lower ligandability than moderately reactive sulfenic acids (Supplementary Fig. 9b).   These collective observations provide further support for the notion that the fragment scaffold drives ligandability, along with the degree of covalent reversibility, as opposed to intrinsic electrophilic reactivity of proteomic sulfenic acids.

Redox-based ligandability by nucleophilic fragments affects the function of diverse proteins.   The SulfenQ analyses herein constitutes the largest human sulfenome dataset so far and, for the first time, reveals its potential for ligandability by nucleophilic fragments (Fig. 4a).   Of these sites, a large fraction of proteins harboring sulfenic acids liganded by fragments in our nucleophilic library has not been recorded in the DrugBank[42] database (70.7%; Fig. 4b). In other words, nucleophilic library members targeted many proteins that currently have no

known means of chemical interrogation. Of DrugBank database proteins with sulfenic acid ligands, 63.6% are characterized as enzymatic, while the non-DrugBank counterparts includes a more diverse classes of proteins (Fig. 4c). Furthermore, among all liganded sites identified in this study, only a small fraction is functionally annotated by UniProt (Fig. 4d). Nucleophilic fragments thus represent a vast wilderness that is ripe for development and functional exploration.
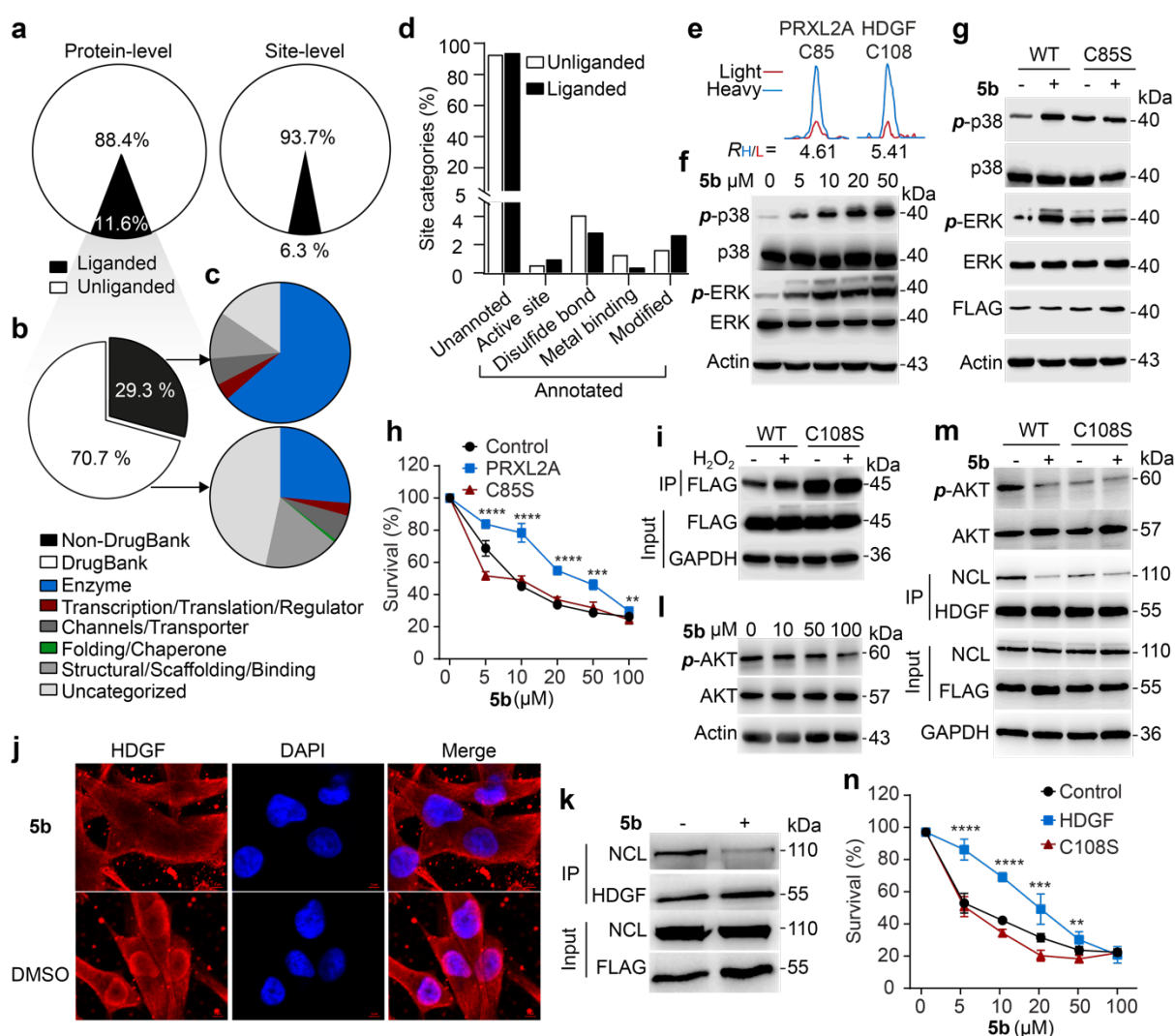
Fig. 4. Redox-based ligandability by nucleophilic fragments affects the function of diverse proteins. a, Pie charts showing the percentage of –SOH sites and proteins liganded by nucleophilic fragments. b, Pie chart showing the percentage of liganded proteins found in DrugBank. c, Functional categorization of DrugBank and non-DrugBank proteins containing liganded –SOH sites. d, Bar chart showing the functional categorization of liganded and unliganded –SOH sites based on cysteine residue annotations retrieved from the UniProt knowledge base. e, Representative XICs showing changes in probe-labeled peptides from PRXL2A and HDGF. The profiles for light- and heavy-labeled peptides are shown in red and blue, respectively. The average $R_{H/L}$ values calculated from biological duplicates are displayed below each XIC. f, Representative western blots showing he activation of MAPK signaling in wild type MDA-MB-231 cells upon the titration of 5b at the indicated concentrations. g, Representative Western blots showing that 5b treatment (50 µM, 2 h) leads to activation of MAPK signaling

17

in MDA-MB-231 cells overexpressing PRXL2A but not its C85S mutant. **h,** Comparison of MDA-MB-231 cell survival rates expressing wild type and C85S mutant PRXL2A upon **5b** treatment, as measured by MTT assay. **i,** Representative Western blots showing that H_2O_2 treatment (0.5 mM, 10 min) leads to an increase of sulfenation on FLAG-tagged HDGF, but not the C108S mutant in MDA-MB-231 cells. **j,** Representative immunofluorescence images showing that **5b** treatment (50 μM, 2 h) inhibited the uptake of HDGF into the nucleus. Scale bar=5 μm. **k,** Representative immunoprecipitation-Western blot results showing that **5b** treatment (50 μM, 2 h) inhibits the HDGF-NCL interaction. Protein binding to heterologously expressed FLAG-HDGF with or without **5b** was subjected to anti-FLAG enrichment, separated with SDS-PAGE and detected with antibodies as indicated for Western blotting. **l,** Representative western blots showing that **5b** titration led to the concentration-dependent decrease of Akt phosphorylation in wild type MDA-MB-231 cells. **m,** Representative Western blots showing that **5b** treatment (50 μM, 2 h) decreased Akt phosphorylation in MDA-MB-231 cells overexpressing HDGF but not its C108S mutant. **n,** Comparison of the survival rates of MDA-MB-231 cells expressing wild type and C108S mutant HDGF upon **5b** treatment, as measured by MTT assay. For (**h**) and (**n**), representative data from biological triplicates are shown; error bars, s.d. Statistical significances were determined by two-sided Student's t-test; **p < 0.01; ***p< 0.001; ****p< 0.0001.

In subsequent studies, we sought to assess the capacity of scout fragment **5b** to modulate the biological function of proteins. Enzymes are a major class of drug targets and were highly enriched in proteins harboring sites liganded by nucleophilic fragments, particularly amongst the DrugBank (Fig. 4c). Covalent reaction of fragment **5b** and liganded active sites would be expected to inhibit enzyme activity. To test this theory, we selected three DrugBank enzymes possessing nucleophilic ligands: GAPDH, GSTO1, and sterol O-acyltransferase 1 (ACAT1, also known as SOAT1). Redox-based GAPDH inhibition has been well documented[43] and was confirmed here by analyzing the effect of H_2O_2 on recombinant protein; oxidation of GSTO1 and ACAT1 similarly inhibited catalytic activity (Supplementary Fig. 10). Enzyme inhibition by H_2O_2 was reversible and could be restored by treatment with dithiothreitol (DTT) indicative of sulfenic acid modification. Incubation of these enzymes with fragment **5b** after oxidation by H_2O_2 precluded recovery of activity with DTT, as expected (Supplementary Fig. 10).

Encouraged by these biochemical findings, we next asked whether and how fragment **5b** might modulate the function of enzymes in cells, particularly those that have not been recorded in the DrugBank. One such protein, peroxiredoxin-like 2A (PRXL2A, also known as PAMM),

caught our attention because it harbors a **5b**-liganded site (C85) within a redox-active CXXC motif (Fig. 4e). PRXL2A is an antioxidant enzyme that counteracts MAPK signaling and the CXXC motif is critical for this inhibitory activity in cells[44]. Interestingly, we found that treatment with fragment **5b** indeed activated MAPK signaling, as shown by upregulated phosphorylation of p38 and ERK in a concentration-dependent manner (Fig. 4f). To establish that this effect is a direct result of C85 liganding by fragment **5b**, we investigated the effect of C85S mutation in MDA-MB-231 cells transfected with a plasmid encoding wild type (WT) or mutant PRXL2A. Notably, this mutation significantly attenuated the activation of MAPK signaling induced by fragment **5b** (Fig. 4g). Also, overexpression of wild type PRXL2A, but not the C85S mutant, increased resistance to cell death induced by **5b** (Fig. 4h), indicating that C85 in the redox-active CXXC motif of PRXL2A mediates, at least in part, the inhibitory activity of this fragment in cells.

We next turned our attention to liganded sites residing on proteins without enzymatic activity, among which HDGF, a well-known oncoprotein[45], is one such example. The cysteine liganded in HDGF by **5b**, C108, is involved in disulfide bond formation; however, whether this site is redox-regulatory remains unknown. We initially investigated the effect of H_2O_2 on HDGF sulfenation in MDA-MB-231 cells by expressing FLAG-tagged wild type HDGF and C108S mutant proteins. Sulfenic acid modification of HDGF in cells increased with exogenous H_2O_2 treatment, as expected, while C108S mutation abolished this effect (Fig. 4i). Interestingly, however, the overall level of HDGF sulfenic acid modification was increased in C108S mutant compared to wild type (Fig. 4i) and likely stems from increased oxidation of

C12 when unpaired with its disulfide partner, C108. Given that HDGF can form a functional complex with nucleolin (NCL)[46], we next asked whether the interaction between **5b** and C108 site could perturb HDGF function through the NCL-Akt pathway[47]. Treatment of cells with **5b** inhibited the uptake of HDGF into the nucleus (Fig. 4j) as well as its interaction with nuclear receptor, nucleolin (NCL; Fig. 4k). Akt phosphorylation, the hallmark of pathway activation, decreased with **5b** treatment in untransfected cells or in those overexpressing HDGF (Fig. 4l, m). HDGF C108S mutation attenuated the inhibitory effect of **5b** on both Akt phosphorylation and the interaction between HDGF and NCL, as well as their basal levels without stimulation (Fig. 4m). Moreover, MDA-MB-231 cells overexpressing HDGF, but not the C108S mutant, exhibited showed an increase in cell survival (Fig. 4n). Taken together, these results suggest that the biological activity of **5b** in cells may be attributed, at least in part, to its inhibitory effect on the HDGF-NCL-Akt axis through binding C108 of HDGF in its oxidized sulfenic acid state.

Discussion

Among all protein coding amino acids, cysteine is the most targeted by electrophilic fragment libraries and thiol-targeted libraries have greatly expanded the proportion of "druggable" space in the human proteome[4,5]. At the same time, it remains challenging to design electrophilic ligands or covalent drugs that react selectively with cysteine targets in the presence of GSH (10 mM)[3,11] and, more importantly, almost 5-fold as many protein thiols[48]. Apart from selenium, sulfur is the most redox-sensitive element in the human proteome and its reactivity with weak electrophiles is significantly diminished, if not abolished, when cysteine sulfur is oxidized[49]. These issues and opportunities have been recognized among both academic and

pharmaceutical scientists[3,50,51] and enthusiasm to exploit differences in cysteine redox to develop novel chemical biology tools and therapeutic strategies continues to grow[19,28,52].

Our nucleophilic fragment library and the analysis presented herein provides a valuable proof-of-concept and highlights the sheer potential of redox-based ligandability of electrophilic sulfur in the human cysteinome.   The SulfenQ method employed in this work, in conjunction with the fragment library, identified more sulfenic acid-modified sites in the human proteome than ever before.   Of these, the vast majority of liganded sites were found in proteins lacking small-molecule probes, including proteins not found in the DrugBank or targeted by cysteine-reactive electrophilic fragments.   We further demonstrated the capacity of nucleophilic fragments to modulate protein function, including inhibition of enzyme activity through active site liganding of GAPDH, GSTO1 and ACAT1 in biochemical studies and PRXL2A in cells.   Furthermore, we have also shown the capacity of a nucleophilic fragment to hinder the interaction between HDGF and its nuclear receptor in cells.

Despite having the same binding scaffold, nucleophilic fragments identified far fewer liganded sites compared to their electrophilic counterparts.   Since only 10-20% of cysteines predicted to be redox-active[53] and sulfenic acid modification is transient in many cases[21] this result was not unexpected.   On this basis, our findings likely indicate the relative selectivity of sulfenic acid modification across the cysteinome and/or the high target preference of nucleophilic fragments tested herein.   Nevertheless, we would be remiss if we did not point out other contributing factors, which may be attributed to technical limitations inherent to SulfenQ.   For

example, the reaction kinetics and target preference of the sulfenic acid probe, BTD likely differ from the two C-nucleophilic warheads used in this study, possibly resulting in an underestimation of competition rates at some sites.   In addition, due to the stochastic nature of data-dependent acquisition-based shotgun proteomics, the proportion of the sulfenome that has the capacity to show interactions with fragment nucleophiles may be under sampled. Future iterations of probes to profile sulfenic acid and improvements in MS (*e.g.,* data-independent acquisition or multiplexed quantification approaches like TMT to reduce missing values across samples and replicates) are fully expected to enhance our ability to comprehensively evaluate the effects of nucleophilic fragment on the sulfenome.

Projecting forward, we envision several interesting pursuits to further expand the ligandability of the human sulfenome.   Analogous to the landmark 2016 study[4] reporting thiol-targeted electrophilic fragments, our library is comprised of fewer than 100 compounds.   The chemical space of our libraries will undoubtedly benefit from the coupling of cyano- and nitroacetamide C-nucleophiles (and other linear and cyclic C-nucleophiles[34,39,54,55]) to an expanded set of fragment amines and to fragments with different linkage types.   More potent, and selective nucleophile fragment-protein interactions may also be achieved through traditional structure-activity-relationship (SAR)-guided approaches.   Bearing in mind that redox processes are context-dependent, future studies will certainly include global comparisons of redox-based ligandability across different cell/tissue types and states.

In summary, nucleophilic fragments that target cysteine in its sulfenic acid state offer a distinct and complementary approach to electrophile-based covalent ligand discovery. The targeting of this redox modification and others like sulfinic acid can be leveraged in future work to develop redox-based chemical probes and pharmaceuticals. More generally, our approach underscores the important, broader effort to discover covalent ligands that target functional groups in proteins beyond thiols, including non-redox post-translational modifications and cofactors[56].

Methods

A detailed Methods section is provided in the Supplementary Information.

Data availability. All data associated with this study are available in the published article and its Supplementary Information. All raw proteomics data will be uploaded to the ProteomeXchange Consortium (http://proteomecentral.proteomexchange.org) via the iProX partner repository with the dataset identifier PXD029761. Source data are provided with this paper.

Author contributions

L.F. designed and performed the chemoproteomic and functional experiments, analyzed data, and drafted the manuscript, Y.J. designed, synthesized, and characterized the nucleophile fragment library, C.T. helped for the functional experiments, R.B.F. synthesized alkyne reporter fragments, F.C.H. acquired funding, J.Y. and K.S.C. conceived the project, supervised the work, analyzed data and the wrote the manuscript with inputs from others.

Competing Interests

The authors declare no competing interests.

References

1.   Singh, J., Petter, R. C., Baillie, T. A. & Whitty, A. The resurgence of covalent drugs. *Nat. Rev. Drug Discov.* **10**, 307–317 (2011).

2.   Békés, M., Langley, D. R. & Crews, C. M. PROTAC targeted protein degraders: the past is prologue. *Nat. Rev. Drug Discov.* **21**, 181–200 (2022).

3.   Lu, W. *et al.* Fragment-based covalent ligand discovery. *RSC Chem. Biol.* (2021) doi:10.1039/d0cb00222d.

4.   Backus, K. M. *et al.* Proteome-wide covalent ligand discovery in native biological systems. *Nature* **534**, 570–574 (2016).

5.   Parker, C. G. *et al.* Ligand and Target Discovery by Fragment-Based Screening in Human Cells. *Cell* **168**, 527-541.e29 (2017).

6. Abbasov, M. E. *et al.* A proteome-wide atlas of lysine-reactive chemistry. *Nat. Chem.* (2021) doi:10.1038/s41557-021-00765-4.

7. Hahm, H. S. *et al.* Global targeting of functional tyrosines using sulfur-triazole exchange chemistry. *Nat. Chem. Biol.* **16**, 150–159 (2020).

8. Zhang, T., Hatcher, J. M., Teng, M., Gray, N. S. & Kostic, M. Recent Advances in Selective and Irreversible Covalent Ligand Development and Validation. *Cell Chem. Biol.* **26**, 1486–1500 (2019).

9. Weerapana, E. *et al.* Quantitative reactivity profiling predicts functional cysteines in proteomes. *Nature* **468**, 790–795 (2010).

10. Bateman, A. *et al.* UniProt: the universal protein knowledgebase in 2021. *Nucleic Acids Res.* **49**, D480–D489 (2021).

11. Zhang, T., Hatcher, J. M., Teng, M., Gray, N. S. & Kostic, M. Recent Advances in Selective and Irreversible Covalent Ligand Development and Validation. *Cell Chem. Biol.* **26**, 1486–1500 (2019).

12. Singh, J. The Ascension of Targeted Covalent Inhibitors. *J. Med. Chem.* (2021) doi:10.1021/acs.jmedchem.1c02134.

13. Li, D. *et al.* BIBW2992, an irreversible EGFR/HER2 inhibitor highly effective in preclinical lung cancer models. *Oncogene* **27**, 4702–4711 (2008).

14. Byrd, J. C. *et al.* Ibrutinib versus Ofatumumab in Previously Treated Chronic Lymphoid Leukemia. *N. Engl. J. Med.* **371**, 213–223 (2014).

15. Nomura, D. K., Dix, M. M. & Cravatt, B. F. Activity-based protein profiling for biochemical pathway discovery in cancer. *Nat. Rev. Cancer* **10**, 630–638 (2010).

16. Vinogradova, E. V. *et al.* An Activity-Guided Map of Electrophile-Cysteine Interactions in Primary Human T Cells. *Cell* **182**, 1009-1026.e29 (2020).

17. Paulsen, C. E. & Carroll, K. S. Cysteine-Mediated Redox Signaling: Chemistry, Biology, and Tools for Discovery. *Chem. Rev.* **113**, 4633–4679 (2013).

18. Meng, J. *et al.* Global profiling of distinct cysteine redox forms reveals wide-ranging redox regulation in C. elegans. *Nat. Commun.* **12**, 1415 (2021).

19. Shi, Y. & Carroll, K. S. Activity-Based Sensing for Site-Specific Proteomic Analysis of Cysteine Oxidation. *Acc. Chem. Res.* **53**, 20–31 (2020).

20. Yang, J., Gupta, V., Carroll, K. S. & Liebler, D. C. Site-specific mapping and quantification of protein S-sulphenylation in cells. *Nat. Commun.* **5**, 4776 (2014).

21. Gupta, V. & Carroll, K. S. Sulfenic acid chemistry, detection and cellular lifetime. *Biochim. Biophys. Acta - Gen. Subj.* **1840**, 847–875 (2014).

22. Truong, T. H. T. H. T. H. *et al.* Molecular Basis for Redox Activation of Epidermal Growth Factor Receptor Kinase. *Cell Chem. Biol.* **23**, 837–848 (2016).

23. Paulsen, C. E. *et al.* Peroxide-dependent sulfenylation of the EGFR catalytic site enhances kinase activity. *Nat. Chem. Biol.* **8**, 57–64 (2012).

24. Heppner, D. E. *et al.* Direct cysteine sulfenylation drives activation of the Src kinase. *Nat. Commun.* **9**, 4522 (2018).

25. Salmeen, A. *et al.* Redox regulation of protein tyrosine phosphatase 1B involves a sulphenyl-amide intermediate. *Nature* **423**, 769–773 (2003).

26. Chiu, J. & Hogg, P. J. Allosteric disulfides: Sophisticated molecular structures enabling flexible protein regulation. *J. Biol. Chem.* **294**, 2949–2960 (2019).

27. Truong, T. H. & Carroll, K. S. Redox regulation of epidermal growth factor receptor signaling through cysteine oxidation. *Biochemistry* **51**, (2012).

28. Forman, H. J. & Zhang, H. Targeting oxidative stress in disease: promise and limitations of antioxidant therapy. *Nat. Rev. Drug Discov.* **20**, 689–709 (2021).

29. Perillo, B. *et al.* ROS in cancer therapy: the bright side of the moon. *Exp. Mol. Med.* **52**, 192–203 (2020).

30. Volpe, C. M. O., Villar-Delfino, P. H., Dos Anjos, P. M. F. & Nogueira-Machado, J. A. Cellular death, reactive oxygen species (ROS) and diabetic complications review-Article. *Cell Death Dis.* **9**, (2018).

31. N. Kolodkin, A. *et al.* ROS networks: designs, aging, Parkinson's disease and precision therapies. *npj Syst. Biol. Appl.* **6**, (2020).

32. Leonard, S. E., Garcia, F. J., Goodsell, D. S. & Carroll, K. S. Redox-based probes for protein tyrosine phosphatases. *Angew. Chemie - Int. Ed.* **50**, (2011).

33. Garcia, F. J. & Carroll, K. S. Redox-based probes as tools to monitor oxidized protein tyrosine phosphatases in living cells. *Eur. J. Med. Chem.* **88**, 28–33 (2014).

34. Gupta, V., Yang, J., Liebler, D. C. & Carroll, K. S. Diverse Redoxome Reactivity Profiles of Carbon Nucleophiles. *J. Am. Chem. Soc.* **139**, 5588–5595 (2017).

35. Fu, L., Liu, K., Ferreira, R. B., Carroll, K. S. & Yang, J. Proteome-Wide Analysis of Cysteine S-Sulfenylation Using a Benzothiazine-Based Probe. *Curr. Protoc. Protein Sci.* **95**, e76 (2019).

36. Shi, Y. & Carroll, K. S. Parallel evaluation of nucleophilic and electrophilic chemical probes for sulfenic acid: Reactivity, selectivity and biocompatibility. *Redox Biol.* **46**,

102072 (2021).

37.   Akter, S. *et al.* Chemical proteomics reveals new targets of cysteine sulfinic acid reductase. *Nat. Chem. Biol.* **14**, 995–1004 (2018).

38.   Petri, L. *et al.* An electrophilic warhead library for mapping the reactivity and accessibility of tractable cysteines in protein kinases. *Eur. J. Med. Chem.* **207**, (2020).

39.   Gupta, V. & Carroll, K. S. Rational design of reversible and irreversible cysteine sulfenic acid-targeted linear C-nucleophiles. *Chem. Commun.* **52**, 3414–3417 (2016).

40.   Fu, L. *et al.* A quantitative thiol reactivity profiling platform to analyze redox and electrophile reactive cysteine proteomes. *Nat. Protoc.* **15**, 2891–2919 (2020).

41.   Crowley, V. M., Thielert, M. & Cravatt, B. F. Functionalized Scout Fragments for Site-Specific Covalent Ligand Discovery and Optimization. *ACS Cent. Sci.* **7**, 613–623 (2021).

42.   Wishart, D. S. *et al.* DrugBank 5.0: A major update to the DrugBank database for 2018. *Nucleic Acids Res.* **46**, D1074–D1082 (2018).

43.   Peralta, D. *et al.* A proton relay enhances H2O2 sensitivity of GAPDH to facilitate metabolic adaptation. *Nat. Chem. Biol.* **11**, 156–163 (2015).

44.   Chen, Y. F. *et al.* miR-125b suppresses oral oncogenicity by targeting the anti-oxidative gene PRXL2A. *Redox Biol.* **22**, 101140 (2019).

45.   Bao, C., Wang, J., Ma, W., Wang, X. & Cheng, Y. HDGF: a novel jack-of-all-trades in cancer. *http://dx.doi.org/10.2217/fon.14.194* **10**, 2675–2685 (2014).

46.   Bremer, S. *et al.* Hepatoma-derived growth factor and nucleolin exist in the same ribonucleoprotein complex. *BMC Biochem.* **14**, (2013).

47.   Shin, S. H. *et al.* Aberrant expression of CITED2 promotes prostate cancer metastasis by activating the nucleolin-AKT pathway. *Nat. Commun.* **9**, (2018).

48.   Hansen, R. E., Roth, D. & Winther, J. R. Quantifying the global cellular thiol-disulfide status. *Proc. Natl. Acad. Sci.* **106**, 422–427 (2009).

49.   Lo Conte, M. & Carroll, K. S. The redox biochemistry of protein sulfenylation and sulfinylation. *J. Biol. Chem.* **288**, 26480–26488 (2013).

50.   Spradlin, J. N., Zhang, E. & Nomura, D. K. Reimagining Druggability Using Chemoproteomic Platforms. *Acc. Chem. Res.* **54**, 1801–1813 (2021).

51.   Maurais, A. J. & Weerapana, E. Reactive-cysteine profiling for drug discovery. *Curr. Opin. Chem. Biol.* **50**, 29–36 (2019).

52.   Sies, H. & Jones, D. P. Reactive oxygen species (ROS) as pleiotropic physiological signalling agents. *Nat. Rev. Mol. Cell Biol.* (2020) doi:10.1038/s41580-020-0230-3.

53.   Go, Y.-M. M., Chandler, J. D. & Jones, D. P. The cysteine proteome. *Free Radic. Biol. Med.* **84**, 227–245 (2015).

54.   Gupta, V. & Carroll, K. S. Profiling the reactivity of cyclic C-nucleophiles towards electrophilic sulfur in cysteine sulfenic acid. *Chem. Sci.* **7**, 400–415 (2016).

55.   Shi, Y., Fu, L., Yang, J. & Carroll, K. S. Wittig reagents for chemoselective sulfenic acid ligation enables global site stoichiometry analysis and redox-controlled mitochondrial targeting. *Nat. Chem.* **13**, 1140–1150 (2021).

56.   Wang, X. *et al.* Discovery of Potent and Selective Inhibitors against Protein-Derived Electrophilic Cofactors. *J. Am. Chem. Soc.* **144**, 5377–5388 (2022).